Preparation of Phenolic Resin/Organized Expanded Vermiculite Nanocomposite and Its Application in Brake Pad

Jianying Yu, Jia He, Chongqing Ya

Key Laboratory for Silicate Material and Engineering of Ministry of Education, Wuhan University of Technology, Wuhan 430070, People's Republic of China

Received 3 July 2009; accepted 28 March 2010
DOI 10.1002/app.32557
Published online 21 July 2010 in Wiley Online Library (wileyonlinelibrary.com).

ABSTRACT: Phenolic resin (PF)/organized expanded vermiculite (OEVMT) nanocomposite was prepared via melt intercalation with EVMT organically treated using benzyldimethyloctadecylammonium. The results of the PF/OEVMT structure characterized by X-ray diffraction and transmission electron microscopy showed that the PF/OEVMT nanocomposite formed exfoliated and intercalated mixed structure. Thermogravimetric analysis indicated that the thermal decomposition temperature of the PF/OEVMT nanocomposite (482.6°C) was higher than that of pristine PF (433.9°C) in air atmosphere. The brake pad based on PF/OEVMT nanocomposite were also prepared. The friction and wear tests illustrated that the brake pad based on PF/OEVMT had more stable friction coefficient and lower wear rate than that of the brake pad based on PF. Scanning electron microscopy also showed that the brake pad based on PF/OEVMT nanocomposite has excellent high temperature wear-resistance. © 2010 Wiley Periodicals, Inc. J Appl Polym Sci 119: 275–281, 2011

Key words: nanocomposite; thermal properties; phenolic resin; vermiculite

INTRODUCTION

In recent years there has been considerable interest in polymer-layered silicate nanocomposites because their use has resulted in improvement in thermal and mechanical properties, even with a small silicate content.[1–3]

Phenolic resin (PF) is produced by the reaction of phenol with aldehyde and it is classified as resol and novolac by synthetic conditions and curing mechanism. Many researches about phenolic resin/layered silicate nanocomposites have been investigated to improve properties of PF. Byun et al.[4] prepared resol type phenolic resin/layered silicate nanocomposites by melt intercalation using various layered silicates such as sodium montmorillonite (MMT) and ω-amino acid modified montmorillonites (C3M, C6M, and C12M). The mechanical properties of the resol type phenolic resin/layered silicate nanocomposites with ω-amino acid modified MMT are better than that of PF/MMT system. This was because the phenolic resin/layered silicate nanocomposites have an end-tethered structure formed by the reaction of the carboxylic acid of the organic modifier with the methylol group of the PF. Pappas et al.[5] synthesized PF/MMT nanocomposites via *in-situ* polymerization. The results showed that the MMT partially exfoliated and the material was mechanically superior. Thermogravimetric analysis (TGA) showed that the addition of MMT improved the thermal stability of the nanocomposites from 210 to 225°C in air atmosphere. Wei et al.[6] prepared PF/MMT nanocomposite using *in-situ* polymerization of resol type phenolic resins with various organo-modified MMTs. It was found that the thermal properties of nanocomposite were enhanced obviously compare to pristine phenolic resin due to favorable interaction between phenolic resin and organic modifiers containing benzene rings.

Like MMT, vermiculite (VMT) is a mica-type silicate, which belongs to the general family of 2 : 1 layered silicates. Each layer consists of octahedrally coordinated cations (typically Mg, Al, and Fe) sandwiched by tetrahedrally coordinated cations (typically Si and Al). The isomorphous substitution of Si^{4+} by Al^{3+} leads to a net negative surface charge that is compensated by an interlayer of exchangeable hydrated cations (Ca^{2+}, Mg^{2+}, Cu^{2+}, Na^{+}, and H^{+}).[7] When pristine VMT flakes are strongly heated at high temperature (≈ 900°C) during a short period of time, the water situated between layers is quickly converted into steams, exerting a disruptive effect upon the structure. As a consequence, a highly porous material named expanded vermiculite (EVMT) is formed and it is an efficient thermal insulator.[8]

Correspondence to: J. Yu (jyyu@whut.edu.cn).

In previous works, Wang et al.[9] prepared polyethylene terephthalate/EVMT nanocomposites via *in-situ* polymerization. The X-ray diffraction (XRD) showed that diffraction peak disappeared and the glass transition temperature of nanocomposites (137.2°C) was higher than that of pure PET (83°C). Han and Liu[10] prepared natural rubber/organized expanded vermiculite (OEVMT) using ball mill method. XRD analysis indicated vermiculite layers dispersed in the nature rubber matrix uniformly. The results of mechanical properties showed that the tensile strength, breaking elongation rate and tear strength of natural rubber were improved greatly. Liu et al.[11] prepared polyaniline/OEVMT nanocomposites via *in-situ* polymerization. It was found that vermiculite layers dispersed in nanoscale and the thermal properties were enhanced. And we have synthesized phenolic resin/organized expanded vermiculite (PF/OEVMT) nanocomposites via melt intercalation.[12] The expanded vermiculite was organically treated by cetyltrimethylammonium bromide (CTAB). The result showed that thermal properties of PF were greatly enhanced. The thermal decomposition temperature of the PF/OEVMT nanocomposite (506°C) were higher than that of pritine PF (445°C) in nitrogen atmosphere.

Phenolic resin is invariably used as binder in brake pad due to its excellent structural integrity, moderate thermal resistance, solvent resistance, and very good wetting capability with most of the ingredients. However, higher heat-resistance and mechanical performance of phenolic resin are required to meet demand of high performance brake pad.[13–16] Sun et al.[17] prepared motor vehicle brake pad using nanosilicon modified phenolic resin. The result showed that the temperature of thermal decomposition of the modified resin was enhanced from 362.3 to 394.3°C in air atmosphere. The high temperature friction coefficient of brake pad based on nanosilicon modified phenolic resin was stable and its heat failing-resistance property was good. Lin et al.[18] prepared phenolic resin modified by nanoparticle copper *in situ* coproducing method. The results indicated that the initially decomposed temperatures of the phenolic resin modified by 7 wt % nanoparticle copper reached to the maximum (335°C) in air atmosphere, 31°C higher than that of pristine PF. The tribological properties of brake pad could be improved by adding the nanoparticles. The heat fade and wear rate could be remarkablely lowered, especially at high temperature. Liu et al.[19] used styrene butadiene nanopowdered rubber for manufacturing brake pads. The results indicated that nanopowdered rubber can substantially improve properties of friction materials, the friction coefficient varies steadily with the change of temperature and the wearing rate of friction materials was relatively low by using nanopowdered rubber. However, there have been few report about brake pad based on phenolic resin/layered silicate nanocomposite till now.

In this study, EVMT modified by benzyldimethyloctadecylammonium (ODBA) was mixed with phenolic resin to form the PF/OEVMT nanocomposite by melt intercalation. Microstructure and thermal properties of the PF/OEVMT nanocomposite were characterized by XRD analysis, transmission electron microscopy (TEM) and TGA. And the brake pads based on PF and the PF/OEVMT nanocomposite was prepared, respectively. Friction and wear behaviour of the brake pads were investigated.

EXPERIMENTAL

Materials

The materials needed in this study were listed in the Table I. The companies which provided these experiment materials were all Chinese companies.

Preparation

Preparation of OEVMT

A total of 10 g EVMT was dispersed in 200 mL deionized water and stirred for 15 min at room temperature. Then combined with 3 g ODBA, this suspension was continuously stirred at 80°C for 12 h to form OEVMT. The OEVMT was separated by filtering and then washed thoroughly with deionized water several times until the absence of halide anions tested with a 0.1*N* $AgNO_3$. The OEVMT, which was dried in a vacuum at 100°C for 3 h, was pulverized in a mortar and sifted through a sieve (300 mesh).

Preparation of PF/OEVMT nanocomposite

Phenolic resin and 2 wt % OEVMT relative to PF (i.e., 98 : 2 PF/OEVMT) were mixed and subsequently stirred at 170°C for 4 h. The product cooled to room temperature was pulverized in a mortar and sifted through the sieve (300 mesh). The PF/OEVMT nanocomposites was obtained.

Preparation of brake pads based on PF and PF/OEVMT nanocomposite

Brake pads based on PF and PF/OEVMT nanocomposite were prepared, respectively. The compositions of the brake pad were showed in the Table II. All these were mixed in the high-speed mixer for 3 min. Filled the moulds with the mixers and press molding in Y7073-300A Hydraulic Machine. The mixers were preserved continuously for 20 min at 160°C under 25 MPa pressure. Then releasd the pressure

TABLE I
Experiment Materials

Name	Detail	Companies
Benzyldimethyloctadecylammonium	Analytical pure	Nanjing Robiot, Co., Ltd.
Expanded vermiculite	250 mesh	Jinli Mineral, Co., Ltd.
Phenolic resin	Thermoplastic phenolic resin	Laiwu Runda Chemical, Co., Ltd.
Hexamethylene tetramine	Analytical pure	
101 cotton	Length of 20–25 mm	Hubei Ace Graphite Technology, Co., Ltd.
Nitrile rubber powder	60 mesh	
Flake graphite	325 mesh, carbon content 95%	
Steel fiber	Diameter of 20–23 μm length of 8–10 mm	Yichang Heyuan Chemical, Co., Ltd.
Aluminum oxide	analytical pure	Sailong Glass Fiber, Co., Ltd.
Glass fiber	Diameter of 15–18 μm, length of 3–5 mm	
Barite	Specific gravity 4.3	Henan Bond Chemical, Co., Ltd.
Cellulose	80 mesh	

and preserved for another 20 min at 160°C. At last, the samples were then cured for 6 h at 150°C.

Testing

X-ray diffraction

The PF/OEVMT nanocomposite was cured with 10 wt % hexamethylene tetramine relative to the phenolic resin (i.e., 90 : 10 phenolic resin/hexamethylene tetramine) at 180°C for 4 h. EVMT, OEVMT, and cured PF/OEVMT were characterized by XRD using a Rigaku D/max 2400 diffractometer with CuKα radiation ($\lambda = 0.154$ nm; 40 kV, 120 mA) at room temperature. The diffractograms were scanned from 1.5° to 10° in the 2θ range in 0.02° steps and scanning rate was 88 min^{-1}.

Transmission electron microscopy

Structure of the cured PF/OEVMT nanocomposite was investigated by means of TEM (Philips Tecnai G2), operated at an accelerating voltage of 200 kV. Sample was embedded in epoxy resin, cured at 60°C overnight and subsequently microtomed at room temperature into ultrathin slices.

Thermogravimetric analysis

The thermal stabilities of the cured PF and the cured PF/OEVMT were measured using a thermal analyzer (TG Instruments, PERKIN-ELMER) with a heating rate of 10°C/min up to 800°C under air flow of 10 mL/min.

Mechanical properties measurements

The rigidity and impact strength of brake pads based on PF and PF/OEVMT separately were measured with XHR-150 Rockwell Apparatus and JC-25 Impact Testing Machine.

Tribological properties measurements

The coefficient of friction and wearing rate of brake pads based on PF and PF/OEVMT separately were tested using XD-MSM Friction Test Machine with temperature range of 100–350°C.The speed of circular disk was 480 r/min and pressure was 0.98 MPa.

Scanning electron microscopy (SEM)

A Quanta 200HV scanning electron microscopy from FEI Company (USA) was used to examine the morphologies of the worn surface of brake pads based on PF and PF/OEVMT after the friction at 350°C.

RESULTS AND DISCUSSION

Morphology of PF/OEVMT nanocomposite

Figure 1 showed the XRD patterns of EVMT, OEVMT, and PF/OEVMT. From Figure 1(a), the EVMT exhibited two diffraction peaks at 2θ = 5.99° and 8.9°. The diffraction peaks at 2θ = 5.99° (d_{001}= 1.48 nm) represented the characteristic d_{001} diffraction peak of EVMT while the peak at 8.9° probably resulted from the impurities within EVMT.[20] As shown in Figure 1(b), the OEVMT gave four distinct peaks at 2θ = 1.9°, 2.5°, 4.9° and 8.9°, corresponding

TABLE II
The Compositions of the Brake Pad

Compositions	Contents (wt %)
PF or PF/OEVMT	42
HMTA	3.6
Cellulose	6
101 Cotton	60
Barite	117
Nitrile rubber powder	9
Graphite	9
Steel fiber	45
Aluminum oxide	6
Glass fiber	12

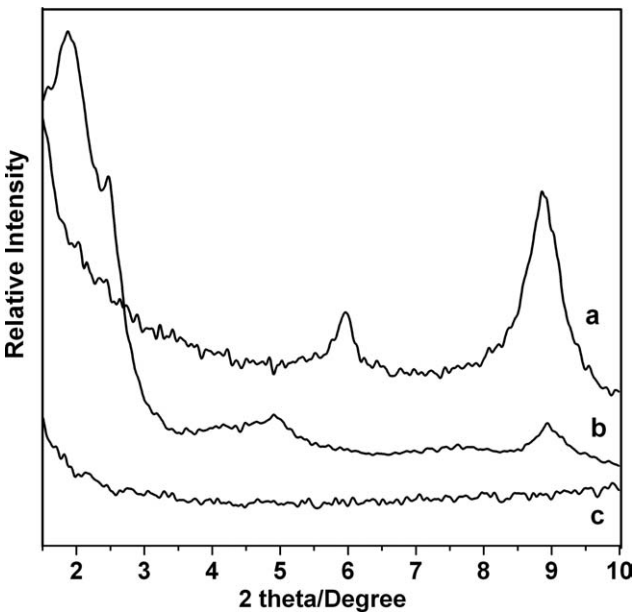

Figure 1 XRD patterns of EVMT, OEVMT, PF/OEVMT nanocomposite. (a) EVMT, (b) OEVMT, (c) PF/OEVMT nanocomposite.

to the d-spacing of 4.55, 3.53, 1.80, 0.99 nm, respectively. It should be noted from the XRD pattern of OEVMT that the interlayer spacing of 4.55, 3.53, 1.80 nm was significantly larger than that of the pristine EVMT. The increase in its interlayer spacing demonstrated ODBA had inserted into the layers of EVMT and it created favourable conditions for PF to get into.

From Figure 1(c), it could be seen that the PF/OEVMT nanocomposite had no evident diffraction peaks in the measured angle scope. As far as microstructure of polymer/layered silicate nanocomposite was concerned, no diffraction peak was visible in the XRD patterns because of too much of large spacing between the layers.[21,22] The absence of the characteristic d_{001} diffraction peak indicated that the spacing between the layers was enlarger and it was more than 5.89 nm (according to $2d \sin \theta = \lambda$, $\theta = 0.75°$).

XRD data alone gives a partial picture of the clay distribution. In the nanocomposite, the dimension and the distribution of layers could be very variable and a complete characterization of the nanocomposite morphology requires also a microscopic investigation.[23] Typical TEM images of PF/OEVMT nanocomposite were shown in Figure 2. In Figure 2(a), most exfoliated vermiculite layers appeared as dark-gray lines. However, a few clusters or stacks of the vermiculite were observed as shown at the arrow. Figure 2(b) showed a magnification image of the clusters or stacks. It was found that a few vermiculites formed intercalated structure. It can be concluded from TEM that the PF/OEVMT nanocomposite formed exfoliated and intercalated mixed structure.

Thermal stability of PF/OEVMT nanocomposite

To identify the nature of thermal degradation encountered when processing nanocomposite at elevated temperatures, thermal gravimetric analysis was performed in air atmosphere. Figure 3 showed the TG curves of the cured PF and PF/OEVMT nanocomposite from room temperature to 800°C. From room temperature to 320°C, there existed some extent weight-loss and the thermal weight-remaining ratio of pristine PF was about 85% at 320°C. Compared to the pristine PF, the thermal weight-loss of the nanocomposite was lower than that of pristine PF and there was almost no thermal weight-loss for PF/OEVMT nanocomposite. The weight remaining ratio of the nanocomposite was about 98.7% at 320°C. The

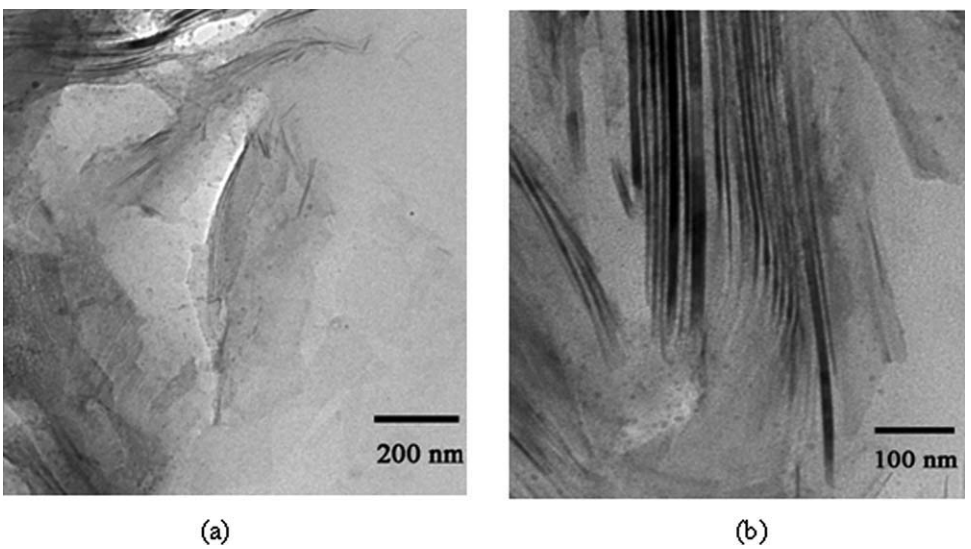

Figure 2 Transmission electron micrographs of PF/OEVMT nanocomposite.

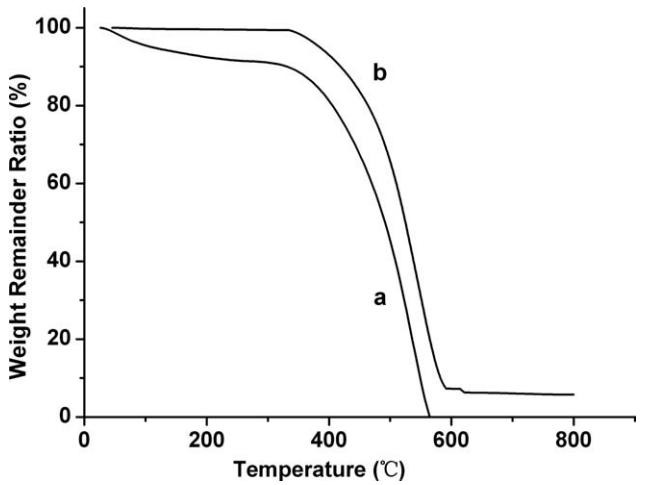

Figure 3 TGA curves of PF and PF/OEVMT nanocomposite in air atmosphere (a) PF, (b) PF/OEVMT.

difference was probably due to the fact that a small amount of low molecular weight PF in the nanocomposite was not easy to volatilize for intercalated and exfoliated structure, which lowered the ratio of thermal weight-loss of the nanocomposite.[22]

When the temperature was more than 400°C, there was notable thermal weight-loss differences between pristine PF and PF/OEVMT. At the same temperature, the nanocomposite had higher weight remainder ratio than pristine PF. When the temperature was 500°C, the weight remainder ratio of pristine PF and PF/OEVMT nanocomposite were 45.8 and 77.1%, respectively. According to the curves, the thermal decomposition temperatures of PF and PF/OEVMT were 433.9 and 482.6°C, respectively. Pristine PF lost weight mainly in the area of 400 to 600°C due to small moleculars like methane, benzaldehyde, phenol, etc. resulted in the oxidation of hydroxyl-terminated and decomposition of free radicals.[24] However, the decomposition of polymer groups was delayed because of the addition of the OEVMT. The vermiculites dispersed in nanoscale could make the conducted route of heat more complex from outside. On the other hand, the silicate platelet may also obstruct loss of permeability of oxygen in the PF matrix by means of their geometrical constraints, and the oxidation of phenolic resin reduced to some extent. Hence the heat-resitance of the pristine PF could be greatly improved by intercalation compounding with organized expanded vermiculite.

Mechanical properties of brake pad based on PF/OEVMT nanocomposite

Table III showed the mechanical properties of brake pads based on PF and PF/OEVMT. From Table III, the impact strength of brake pad based on PF/OEVMT increased by 12% compared to brake pad based on PF. This may be because that the vermiculites of the high aspect ratio dispersed in the phenolic matrix at the nanoscale level acted as the fibers and could stopped the crack outspreading under the external force. Again according to Table III, it was found that the rockwell rigidity was decreased from 22 to 20 due to addition of OEVMT. The decrease of rigidity was not only propitious to protect the friction couple materials from abrasion, but also reduce the noisy.

TABLE III
The Mechanical Properties of Brake Pads based on PF and PF/OEVMT

Kinds of brake pad	Impact strength (dJ/cm^2)	Rockwell rigidity (HRC)
Brake pad based on PF	4.32	22
Brake pad based on PF/OEVMT	4.85	20

Tribological properties of brake pad based on PF/OEVMT nanocomposite

Figure 4 showed the friction coefficient of the brake pads changed with the temperature. From Figure 4(a), in the range of 100–300°C, the friction coefficient of brake pad based on PF increased with the temperature rising. At 300°C, the friction coefficient reached the highest with the value of 0.54. After this, the friction coefficient of brake pad based on PF decreased sharply from 0.54 to 0.30 from 300 to 350°C. However, the friction coefficient of brake pad based on PF/OEVMT was stable during test temperature range in Figure 4(b). From 100 to 200°C, the friction coefficient increased a little from 0.48 to

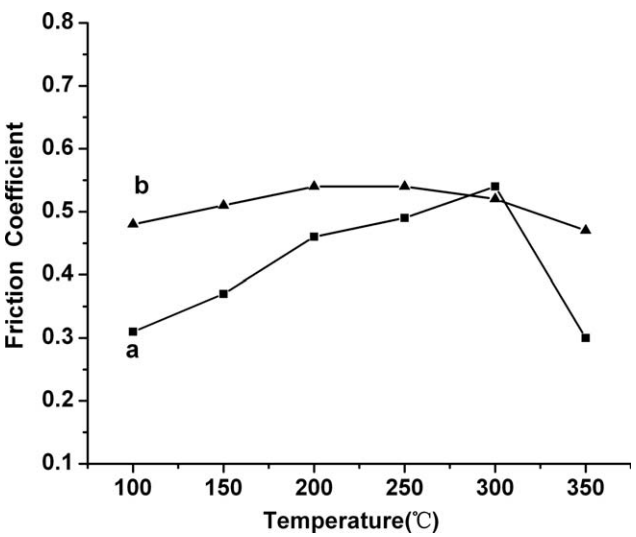

Figure 4 Friction coefficient curves of brake pads based on PF and PF/OEVMT (a) brake pad based on PF, (b) brake pad based on PF/OEVMT.

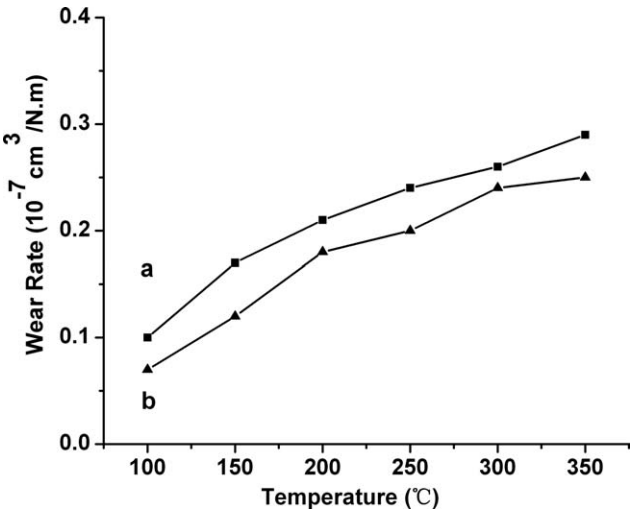

Figure 5 Wear rate curves of brake pads based on PF and PF/OEVMT (a) brake pad based on PF, (b) brake pad based on PF/OEVMT.

0.53. Above 200°C, the friction coefficient recorded a slightly decrease from 0.53 to 0.47. And during sensitive thermal fade extent 300–350°C, it only reduced from 0.52 to 0.47.

The friction coefficient of the brake pads based on PF and PF/OEVMT changes with temperature were closely related with different thermal properties of PF and PF/OEVMT. It could be noted that the increase of friction coefficient of brake pad based on PF in Figure 4(a) responsed to a certain extent decomposition of pristine PF in Figure 3(a). At 300°C, the weight loss of pristine PF was about 10% according to Figure 3(a). The decomposition of pristine PF would result in the lots of wear particles that could make the surface of brake pad based on PF rough. Hence the friction coefficient of brake pad based on PF was enhanced from 100 to 300°C. After 300°C, the pristine PF began to decompose obviously and the serious decomposition of PF caused fillers breaking off. Therefore the friction coefficient decreased sharply as the Figure 4(a) showed.

However, compared with the pristine PF, thermal property of PF/OEVMT was enhanced and there was no evident thermal weight-loss before 350°C. In the Figure 3(a), the weight-loss of PF/OVEMT was only about 1.72% at 300°C. Even at 350°C, the weight-loss of PF/OVEMT was only about 4.72%. Therefore, the PF/OEVMT kept stable basically and may only melt down instead of decomposing. Wear particles were much less and the friction interface was smooth, so the friction coefficient of brake pad based on PF/OEVMT didn't change much.

Figure 5 showed that wear rate of the brake pads changed as temperature. From Figure 5, both wear rates of these two kinds of brake pad were increased with the temperature raised. In Figure 5(a), the wear rate of brake pad based on PF was increased from 0.1×10^{-7}cm^3/N m to 0.29×10^{-7}cm^3/N m from 100 to 350°C. However, the wear rate of brake pad based on PF/OEVMT was lower than that of brake pad based on PF in Figure 5(b). The wear rate of brake pad based on PF/OEVMT was increased from 0.07×10^{-7} cm^3/N m to 0.25×10^{-7}cm^3/N m from 100 to 350°C. This may also be attributed to high thermal decomposition temperature of PF/OEVMT nanocomposite.

Surface morphology of brake pads after friction

Figures 6 and 7 respectively showed the surface morphology of brake pads based on PF and PF/OEVMT after the friction at 350°C. Observing Figure 6(a), there was plenty of scrappy abrasive dusts adhering to the friction surface. From Figure 6(b), the granule broke off from the surface and the steel fiber was pulled out due to the decomposition of PF at high temperature, which directly weaken the bond force among the resin, fillers, and fiber. Comparatively, there were no obvious furrow, dent, wear particle on the surface of the brake pad in Figure 7(a), and the fiber was embeded by the thin film in Figure 7(b), which indicated that resin in brake pad based on PF/OEVMT undecomposed at high temperature.

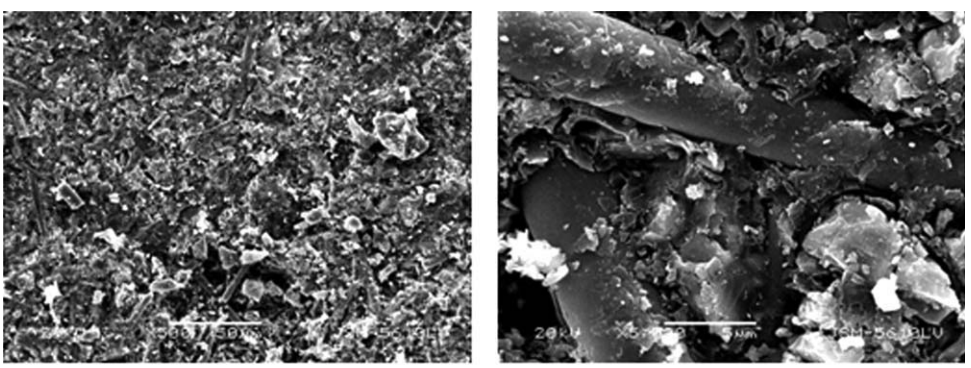

Figure 6 Surface morphology of brake pad based on PF after friction at 350°C in different magnifications.

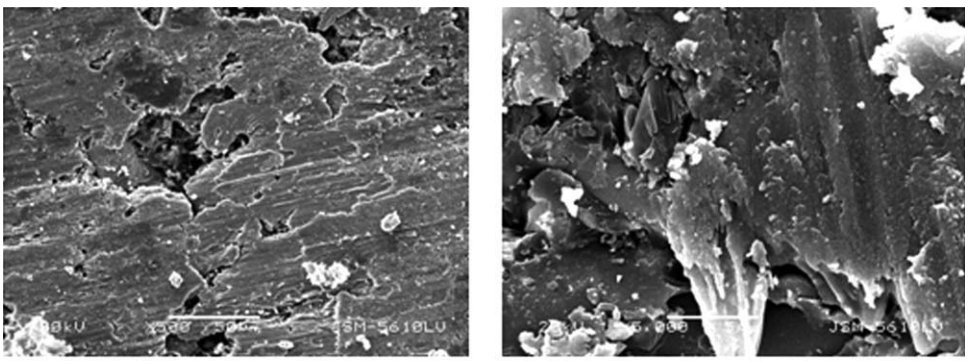

Figure 7 Surface morphology of brake pad based on PF/OEVMT after friction at 350°C in different magnifications.

CONCLUSIONS

PF/OEVMT nanocomposite was successfully prepared via melt intercalation using expanded vermiculites modified with ODBA. XRD and TEM examinations showed that the PF/OEVMT nanocomposite formed exfoliated and intercalated mixed structure. TGA indicated that the PF/OEVMT nanocomposite exhibited excellent thermal properties. The thermal decomposition temperature of the PF/OEVMT nanocomposite reached 482.6°C in air atmosphere, 48.7°C higher than that of pristine PF. Compared with 45.8% weight remainder ratio of PF, the weight remainder ratio of the PF/OEVMT nanocomposite reached 77.1% at 500°C.

The mechanical properties and the friction and wear properties of the brake pad based on PF/OEVMT nanocomposite were investigated. The impact strength of brake pad based on PF/OEVMT were improved. Compared with brake pad based on PF, brake pad based on PF/OEVMT had more stable friction coefficient and lower wear rate. The friction coefficient of brake pad based on PF/OEVMT only decreased 0.05 from 300 to 350°C, while reduced 0.24 for brake pad based on PF. SEM showed that the granule shed from the surface of brake pad based on PF and the steel fiber was pulled out after high temperature friction. However, there were no obvious furrow, dent, wear particle on the surface of brake pad based on PF/OEVMT and the fiber was embeded by the thin film. The high temperature wear-resistance of brake pad based on PF/OEVMT was significantly enhanced.

The authors thank all the research staff in the Center for Materials Research and Analysis of Wuhan University of Technology for the characterization and testing.

References

1. Choi, M. H.; Chung, I. J. J Appl Polym Sci 2003, 90, 2316.
2. Siddiqui, N. A.; Woo, R. S. C.; Kim, J. K.; Leung, C. C. K.; Munir, A. Compos A 2007, 38, 449.
3. Subramaniyan, A. K.; Sun, C. T. Compos A 2006, 37, 2257.
4. Byun, H. Y.; Choi, M. H.; Chung, I. J. Chem Mater 2001, 13, 4221.
5. Pappas, J.; Patel, K.; Nauman, E. B. J Appl Polym Sci 2005, 95, 1169.
6. Wei, J.; Chen, S. H.; Chen, Y. J Appl Polym Sci 2006, 102, 5336.
7. Du, X. S.; Xiao, M.; Meng, Y. Z. Polym Int 2004, 789.
8. Shelly, D. B.; Hsien, C. W.; Emmanuel, P. G. Chem Mater 1999, 11, 1055.
9. Wang, K.; Zhu, Z.; Guo, B. N. Chin J Appl Chem 2003, 20, 709.
10. Han, W.; Liu, W. Acta Mater Compos Sin 2006, 23, 77.
11. Liu, D. F.; Du, X. S.; Meng, Y. Z. Mater Lett 2006, 60, 1847.
12. Yu, J. Y.; Wei, L. Q.; Cao, X. K. J Mater Eng 2004, 4, 20.
13. Gurunath, P. V.; Bijwe, J. Wear 2007, 263, 1212.
14. Yeh, M. K.; Tai, N. H.; Lin, Y. J. Mater Sci Forum 2006, 505, 121.
15. Su, F. H.; Zhang, Z. Z.; Guo, F.; Men, X. H.; Liu, W. M. Compos Sci Technol 2007, 67, 981.
16. Hong, U. S.; Junga, S. L.; Choa, K. H.; Choa, M. H.; Kim, S. J.; Janga, H. Wear 2009, 266, 739.
17. Sun, Z. Y.; Hu, C.; Lei, S. M.; Gong, W. Q. Non-Metallic Mines 2004, 27, 51.
18. Lin, R. H.; Xi, Y. X.; Shao, Y. X.; Fang, L. J Xi'an Jiaotong University 2004, 38, 1203.
19. Liu, Y. Q.; Fan, Z. Q.; Ma, H. Y.; Tan, Y. G.; Qiao, J. L. Wear 2006, 261, 225.
20. Xu, J.; Meng, Y. Z.; Xu, Y.; Rajulu, A. V. J Polym Sci 2003, 41, 749.
21. Kornmann, X.; Lindberg, H.; Berglund, L. A. Polymer 2001, 42, 1303.
22. Fornes, T. D.; Hunter, D. L.; Paul, D. R. Polymer 2004, 45, 2321.
23. Takahashi, S.; Goldberg, H. A.; Feeney, C. A.; Karim, D. P. Polymer 2006, 47, 3083.
24. Srikhirin, T.; Moet, A.; Jerome, B. Polym Adv Technol 1998, 9, 491.